

Reviewer #3

Eurasian autumn snow impact on winter North Atlantic Oscillation depends on cryospheric variability

The manuscript has been improved. I have two remaining issues that may be addressed by the authors.

1) If the purpose of the study is not to determine any sort of causality, then I think the manuscript title should be changed to reflect this. I also think the authors should check through the text to ensure that causality is not inferred.

REPLY: Thank you very much for your comment. In order to reduce the amount of inferred causality linguistically, we changed the title of the manuscript to Eurasian autumn snow link to winter North Atlantic Oscillation strongest for Arctic warming periods. Moreover, we changed specific wording like „impact“ or „connection“ throughout the document, especially so in the discussion section.

2) Conclusions from Fig. 6 are quite speculative. I don't know what critical information this figure has conveyed. Does this figure support the key messages?

REPLY: Thank you very much for your comment. Indeed, the value of the information in terms of dynamics is not very high for Figure 6. However, we think it has some value in conveying the time evolution of different climate indices over the last 130 years in a very quick and convenient way, rather than just explaining that time evolution in text. Nevertheless, we deleted the time series for the ENSO evolution, since we do not discuss that relationship in detail. With this, the Figure is more concise and acts as a visual guide for the reader. As such, we decided to keep Figure 6 in the manuscript.

Reviewer #2

The authors have well taken into account my comments. I suggest acceptance of the manuscript after the following technical corrections:

Line 86: more powerful than what? I guess sea ice, but make it clear.

REPLY: Added information accordingly. Yes, we meant sea ice.

Line 100: seem

REPLY: Fixed

Line 119: snow cover

REPLY: Fixed

Line 449: onwards: use past tense systematically when describing what was done.

REPLY: We now use past tense systematically for the discussion section

Line 502: impacted by what?

REPLY: Added explanation as to what is impacted by which phenomenon

Line 557: drop comma

REPLY: Fixed

Line 600: drop “a”

REPLY: Fixed

List of relevant changes:

- 1) Title change
- 2) Exchanged vocabulary that supported causality

Eurasian autumn snow [link to](#) winter North Atlantic Oscillation strongest for Arctic warming periods

Martin Wegmann (1), Marco Rohrer (2,3,*), Maria Santolaria-Otín (4) and Gerrit Lohmann (1)

(1) Alfred Wegener Institute, Helmholtz Centre for Polar and Marine Research, Bremerhaven, Germany

(2) Oeschger Centre for Climate Change Research, University of Bern, Bern, Switzerland

(3) Institute of Geography, University of Bern, Bern, Switzerland

(4) Institut des Géosciences de l'Environnement, Université Grenoble-Alpes, France

(*) now at: Axis Capital, Zurich, Switzerland

Abstract:

In recent years, many components of the connection between Eurasian autumn snow cover and wintertime North Atlantic Oscillation (NAO) were investigated, suggesting that November snow cover distribution has strong prediction power for the upcoming Northern Hemisphere winter climate. However, nonstationarity of this relationship could impact its use for prediction routines. Here we use snow products from long-term reanalyses to investigate interannual and interdecadal links between autumnal snow cover and atmospheric conditions in winter. We find evidence for a negative NAO-like [signal](#) after November with a strong west-to-east snow cover gradient, which is valid throughout the last 150 years. This correlation is linked with a consistent [link](#) of November snow [to](#) the stratospheric polar vortex [state](#). Nevertheless, interdecadal variability for this link shows episodes of decreased correlation strength, which co-occur with episodes of low variability in the November snow index. On the contrary, periods with high prediction skill for winter NAO are found in periods of high November snow variability, which co-occur with the Arctic warming periods of the 20th century, namely the early 20th century Arctic warming between 1920-1940 and the ongoing anthropogenic global warming at the end of the 20th century. A strong snow dipole itself is consistently associated with reduced Barents-Kara sea ice concentration, increased Ural blocking frequency and negative temperature anomalies in eastern Eurasia.

Keywords: SNOW, NAO, SEA ICE, VARIABILITY, PREDICTION

Deleted: impact on

Deleted: impact

Deleted: impact

Deleted: on

1. Introduction

As the leading climate variability pattern affecting winter climate over Europe (**Thompson and Wallace 1998**), the North Atlantic Oscillation (NAO) has been extensively studied over the last decades (**Wanner et al., 2001; Hurrell and Deser 2010; Moore and Renfrew 2012; Pedersen et al., 2016; Deser et al., 2017**). The NAO has been defined as the variability of the pressure gradient between Iceland (representing the edge of the polar front) and the Azores (representing the subtropical high ridge). The sign of the NAO is related to weather and climate patterns stretching from local to continental scales. Since its variability has severe socioeconomic, ecological and hydrological impacts for adjacent continents, seasonal to decadal predictions of the state of the winter NAO are high-priority research for many climate science centers (**Jung et al., 2011; Kang et al., 2014; Scaife et al., 2014; Scaife et al., 2016; Smith et al., 2016; Dunstone et al., 2016; Wang et al., 2017; Athanasiadis et al., 2017**).

Together with the rapid warming of the Arctic and the increased frequency of severe winters over Eurasia and North America (**Yao et al., 2017; Cohen et al., 2018; Kretschmer et al., 2018; Overland and Wang 2018**), recent studies highlighted the state of the Northern Hemispheric cryosphere as a useful predictor for the boreal wintertime (DJF) NAO (**Cohen et al., 2007; Cohen et al., 2014; Vihma 2014; Garcia-Serrano et al., 2015; Cohen 2016, Orsolini et al., 2016; Crasemann et al., 2017; Warner 2018**). Although both systems seem to be connected (**Cohen et al., 2014; Furtado et al., 2016; Gastineau et al., 2017**), the emerging main hypothesis connects reduced autumn Barents-Kara sea ice concentration and increased Siberian snow cover with a negative NAO state in the following winter months (**Cohen et al., 2014**).

The proposed mechanism behind this hypothesis is a multi-step process, starting with autumn sea ice loss for the European Arctic, followed by altered tropospheric circulation due to elevated Rossby wave numbers, vertical propagation of said Rossby waves upward into the stratosphere and consequently a weakening of the polar vortex (see **Cohen et al., 2014** for an in depth discussion). With the weakening (or the reversal) of the polar vortex, a stratospheric warming signal manifests. This signal propagates slowly back into the troposphere, where it manifests itself as a negative NAO, connected to the concurrent cold winters for Eurasia (**Kretschmer et al., 2018**).

68 In recent years, many components of this pathway were investigated, especially concerning
69 the increased frequency of cold winters over Europe and the emergence of the counter-
70 intuitive “Warm Arctic – cold continent” (WACC) pattern over Eurasia (Petoukhov and
71 Semenov 2010; Vihma 2014). However, there remains substantial uncertainty about the
72 impact of Arctic sea ice in terms of location (Zhang et al., 2016; Luo et al., 2017; Screen
73 2017; Kelleher and Screen 2018), timing (Honda et al., 2009; Overland et al., 2011; Inoue
74 et al., 2012; Suo et al., 2016; Sorokina et al., 2016; King et al., 2016; Screen 2017;
75 Wegmann et al., 2018a; Blackport and Screen 2019) or if sea ice can be used as a
76 predictor/forcing at all based on the contrasting result of model studies (McCusker et al.,
77 2016; Collow et al., 2016; Pedersen et al., 2016; Boland et al., 2017; Crasemann et al.,
78 2017; Ruggieri et al., 2017; Garcia-Serrano et al., 2017; Francis 2017; Screen et al.,
79 2018; Mori et al., 2019; Hoshi et al., 2019; Blackport et al., 2019; Romanowksy et al.,
80 2019).

81 The interplay between Arctic sea ice and Siberian snow is much less explored. Ghatak et al.
82 (2010) showed that reduced autumn polar sea ice leads to the emergence of increased Siberian
83 winter snow cover, especially so in the eastern part of Eurasia. This dipole signal was
84 amplified in coupled climate model runs for the 21st century, where sea ice is substantially
85 diminished. In an observational study, Yeo et al. (2016) point out that the moisture influx
86 from the open Arctic ocean into the Eurasian continent contributes to the increase of snow
87 cover, a mechanism described by Wegmann et al. (2015). Gastineau et al. (2017) found that
88 reduced sea ice is connected to a distinct November snow dipole over Eurasia, both in
89 reanalysis and model data. They further state that the snow component is a statistically more
90 powerful predictor than sea ice for the atmosphere in the following winter. This relationship
91 was also found in a range of climate models, albeit with weaker links. Xu et al. (2019) found
92 the same correlation in observational and model data, however looking at winter climate only.
93 Based on their analysis, the authors state that the enhanced snow cover in winter is a product
94 of the negative NAO rather than a precursor. Sun et al. (2019) highlight the importance of
95 elevated North Atlantic sea surface temperatures for the development of a Eurasian snow
96 dipole in autumn. This warming of the North Atlantic favors reduced sea ice cover for the
97 European part of the Arctic, which triggers a high pressure anomaly over the Northern Ural
98 Mountains via increased ocean to atmosphere heat fluxes, transporting cold air masses
99 towards the south of its eastern flank.

100 The possible impact of the Siberian snow on the stratosphere and eventually on the NAO is
 101 well discussed in **Henderson et al. (2018)**. Although observational NAO prediction studies
 102 with Siberian snow showed great success in the past (**Cohen and Entekhabi 1999; Saito et**
 103 **al., 2001; Cohen et al., 2007; Cohen et al., 2014; Han and Sun 2018**), links between snow
 104 and the stratosphere still seem to be missing or too weak in model studies (**Furtado et al.,**
 105 **2015; Handorf et al., 2015; Tyrrell et al., 2018; Gastineau et al., 2017; Peings et al.,**
 106 **2017**), whereas nudging realistic snow changes to high resolution models seems to improve
 107 the prediction skill (**Orsolini and Kvamsto 2009; Orsolini et al., 2016; Tyrrell et al., 2019**).
 108 Moreover, even though the stratosphere–surface connection is now reasonably well
 109 established (**Kretschmer et al., 2018**), the timing and location of the snow cover used for the
 110 prediction is, as with sea ice, still debated (**Yeo et al., 2016; Gastineau et al., 2017**). As an
 111 additional caveat, **Peings et al. (2013)** and more recently **Douville et al. (2017)**, showed that
 112 the proposed autumn snow-to-winter NAO relationship is non-stationary for the 20th century.
 113 A possible modulator for that relationship might be the phase of the Quasi Biennial
 114 Oscillation (QBO) (**Tyrrell et al., 2018; Peings et al., 2017; Douville et al., 2017**). **Peings**
 115 **(2019)** argues that neither snow nor sea ice anomalies trigger the stratospheric conditions
 116 needed to produce winter extremes and that instead high tropospheric blocking frequency
 117 over Northern Europe leads to the cryosphere anomalies.

118 Here, we follow up on the definition of a November Eurasian snow cover dipole (**Ye and Wu**
 119 **2017; Gastineau et al., 2017; Han and Sun 2018**) which was identified to provide predictive
 120 power for the following winter months at the end of the 20th century. It is however unclear if
 121 this prediction skill is stable for time periods further back than 30 years and how it evolves in
 122 periods of high Arctic sea ice cover. In this study we address the question of a)
 123 nonstationarity of the Eurasian snow cover to winter European surface climate relationship in
 124 the 20th century, b) importance of snow versus sea ice as predictor and c) possible
 125 precursors/modulators of the sea ice–snow–stratosphere chain. With this we aim to contribute
 126 to the understanding of impacts of cryosphere variability on midlatitude circulation (**Francis**
 127 **2017; Henderson et al., 2018; Cohen et al; 2019**). To this end, we utilize centennial
 128 reanalyses and reconstruction data, where we focus on the transition from October to
 129 November to DJF to facilitate the idea of seasonal prediction.

130 This paper is organized as follows: Section 2 describes the data and methods used. In section
 131 3, we introduce the snow cover indices and their interannual prediction value. Section 4
 132 investigates interdecadal shifts in the correlation between snow cover and NAO as well as

Deleted: s

possible determining factors. The results are discussed in section 5 and finally summarized in section 6.

2. Data and Methods

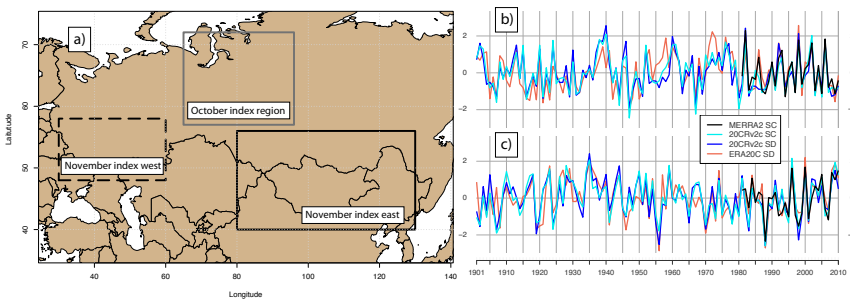
a. Atmospheric reanalyses

To evaluate long-term reanalyses, we use snow cover, snow depth and atmospheric properties from the MERRA2 reanalysis (Gelaro et al., 2017). MERRA2 has a dedicated land surface module and was found to reproduce local in-situ snow conditions over Russia very well (Wegmann et al., 2018b). For a detailed description of how MERRA2 computes snow properties see e.g. Orsolini et al., (2019).

To cover the 20th century and beyond, we include two long-term reanalyses in this study, namely the NOAA-CIRES 20th century reanalysis Version 2c (20CRv2c) (Cram et al., 2015) as well as the Centre for Medium-Range Weather Forecasts (ECMWF) product ERA-20C (Poli et al., 2016). From the ERA-20C product we use snow depth, whereas from 20CRv2c we investigate snow depth and snow cover. Both reanalyses were found to represent interannual snow variations over Eurasia remarkably well. For an in-depth discussion of their performance and their technical details concerning snow computation see Wegmann et al., (2017). We also performed the same analysis using the coupled ECMWF reanalysis CERA-20C (Laloyaux et al., 2018), but found no added knowledge gain over ERA-20C. Thus, we do not include CERA-20C in any further analysis.

We use detrended anomalies of these three reanalysis products to extend the October and November index proposed by Han and Sun (2018) into the past, where the November index is in essence the snow dipole described by Gastineau et al. (2017) using maximum covariance analysis (Figure 1). Where the October index is just calculated as field average snow cover, the November index is computed as difference between the eastern and the western field average. It should be noted, that Han and Sun (2018) found the November index to be linked to a negative NAO and colder Eurasian near-surface temperatures, whereas the October index was correlated with warmer-than-usual temperatures over Eurasia and a southward-shifted jet. However, since many studies focus on Northern Eurasian October snow cover as the predictor for winter climate, we will include it nonetheless. MERRA2 and 20CRv2c offer snow cover as well as snow depth as a post-process output, however ERA-20C only offers snow depth. We refrain from converting it to snow cover ourselves, but found

165 the index based on snow depth to be extremely similar (also see Supplementary Figure 1) to
 166 the same index using snow cover. Moreover, comparing snow indices from reanalyses with
 167 snow indices using the NOAA Climate Data record of Northern Hemisphere Snow Cover
 168 extent (**Robinson et al. 2012**), which incorporates satellite data, does not highlight any
 169 meaningful differences (Supplementary Figure 2). All snow indices are normalized and
 170 linearly detrended with respect to their overall time period. Generally, we found the long term
 171 reanalyses to be of comparable quality of MERRA2 during the overlapping periods.



172 Figure 1: a) Regions for October and November snow index used in this study. b) Linearly
 173 detrended and standardized October snow index comparison for the 20th century for snow
 174 cover (SC) and snow depth (SD) variables. c) same as b) but for the November snow dipole.

176 Besides snow properties we use detrended atmospheric and near-surface anomaly fields from
 177 all three reanalyses. Moreover, as **Douville et al. (2017)**, we use the field averaged (60°–90°
 178 N) 10 hectopascal (hPa) geopotential height (GPH) anomalies in ERA-20C as a surrogate for
 179 polar vortex (PV) strength. Although ERA-20C only assimilates surface pressure, correlation
 180 between this stratospheric index in ERA-20C and MERRA2 during the overlapping time
 181 periods is higher than 0.9.

182 The ERA20C 10 hPa November–December mean GPH shows remarkable interannual
 183 agreement with state-of-the-art reanalyses that assimilate upper air data for the period 1958–
 184 2010 (see Supplementary Figure 3). Moreover, MERRA2 and ERA20C 10 hPa GPH
 185 anomalies agree best over the northern polar regions with correlation coefficients of >0.9 for
 186 the period 1981–2010 (see Supplementary Figure 3). This fact supports the extended value of
 187 the ERA20C polar stratosphere. Before 1958, the quality of the ERA20C stratosphere is
 188 difficult to assess, but the comparison with reconstructions of 100 hPa GPH zonal means
 189 shows very good agreement for late autumn and winter months (see Supplementary Figure 4).

190 As the 20CRv2c ensemble mean dilutes the interannual variability signal back in time with
 191 increased variability within the ensemble members, we use the deterministic run of ERA20C
 192 for the following stratosphere analyses.

193 We use 6-hourly 500 hPa GPH fields (GPH500) to calculate monthly blocking frequencies
 194 according to **Rohrer et al. (2018)**. Blockings are computed according to the approach
 195 introduced by **Tibaldi and Molteni (1990)** and are defined as reversals of the meridional
 196 GPH500 gradient. In accordance to **Scherrer et al. (2006)** the one-dimensional **Tibaldi and**
 197 **Molteni (1990)** algorithm is extended to the two dimensions by varying the latitude between
 198 35° and 75° instead of a fixed latitude:

199 i) GPH500 gradient towards pole: $GPH500G_P = \frac{GPH500_{\varphi+d\varphi} - GPH500_{\varphi}}{d\varphi} < -10 \frac{m}{^{\circ}lat}$ (1)
 200

201 ii) GPH500 gradient towards equator: $GPH500G_E = \frac{GPH500_{\varphi} - GPH500_{\varphi-d\varphi}}{d\varphi} > 0 \frac{m}{^{\circ}lat}$ (2)
 202

203 Blocks by definition are persistent and quasi-stationary high-pressure systems that divert or
 204 severely slow down the usually prevailing westerly winds in the mid-latitudes. They influence
 205 regional temperature and precipitation patterns for an extended period. Therefore, not all
 206 blocks that fulfill the two above-mentioned two conditions are retained. We only include
 207 blocks that have a minimum required lifetime of 5 days and a minimum overlap of the
 208 blocked area of 70% ($A_{t+1} \cap A_t > 0.7 * A_t$) in our blocking catalog. This largely follows the
 209 criteria defined by **Schwierz et al. (2004)**.

210 b) Climate reconstructions

211 To be as independent as possible with regards to the reanalyses we use a wide array of climate
 212 index reconstructions for the 20th century:

- 213 • Atlantic Multidecadal Oscillation (AMO): For the AMO index we take October values
 214 based on the **Enfield et al. (2003)** study. We choose October to allow for a certain
 215 feedback lag with the atmosphere and to have decent prediction value for the
 216 upcoming snow and NAO indices.
- 217 • El Niño – Southern Oscillation (ENSO): We chose the ENSO3.4 reconstruction based
 218 on the HadISSTv1 **Rayner et al. (2003)** SSTs. As with the AMO, we select October
 219 values to allow for a reaction time in the teleconnections.

- North Atlantic Oscillation (NAO): We use the extended **Jones et al. (1997)** NAO index for DJF from the Climate Research Unit (CRU).
- Sea Ice: We use the monthly sea ice reconstruction by **Walsh et al. (2017)** which covers the period 1850–2013 to create a Barents-Kara (65–85°N, 30–90°E) sea ice index for November.

We checked for autocorrelation in the time series of the snow indices, stratospheric index, BKS sea ice index (Supplementary Figure 5), AMO index and ENSO index and only found significant autocorrelation in the BKS sea ice and AMO time series. We assess the significance of a regression coefficient in a regression model by dividing the estimated coefficient over the standard deviation of this estimate. For statistical significance we expect the absolute value of the t-ratio to be greater than 2 or the P-value to be less than the significance level ($\alpha=0.05$). The df are determined as (n-k) where as k we have the parameters of the estimated model and as n the number of observations.

3. Results

a. Interannual links

In the following paragraphs we investigate the year-to-year relationship between the snow indices and the following winter SLP fields. For this we use MERRA2 for a 35-year-long period ranging from 1981–2015, ERA20C for a 110-year-long window ranging from 1901–2010 and 20CRv2c for a 160-year-long window ranging from 1851–2010.

Figure 2 shows the linear regression fields of DJF SLP anomalies projected onto the respective snow indices in October and November. For October, we find no NAO-like pressure anomaly appears to be significantly correlated with the snow index in each of the three reanalysis products and respective time windows (Figure 2a,b,c). Instead, negative SLP anomalies dominate Northern Eurasia in MERRA2, with high pressure anomalies towards the Himalayan Plateau. The 110-year-long regression in ERA20C shows significant negative anomalies over the Asian part of Russia, reaching as far south as Beijing. A second significant negative SLP pattern appears along the Pacific coast of Canada. Finally, SLP anomalies in 20CRv2c support the main SLP patterns shown by ERA20C, but reduce the extent of negative

250 anomalies over Eurasia and increase the extent of the negative anomalies over the North
251 Pacific.

252 The DJF SLP anomaly patterns change substantially when projected onto the November snow
253 index (Figure 2d,e,f). All three reanalysis products show negative NAO-like pressure
254 anomalies with significantly positive anomalies over Iceland and the northern North Atlantic
255 and significantly negative anomalies south of ca. 45° N, including Portugal and the Azores.
256 As expected, MERRA2 shows the strongest anomalies due to the shorter regression period,
257 however interestingly ERA20C, with the 110-year long analysis period, shows less large-
258 scale significance for positive anomalies in high latitudes compared to the 150-year-long
259 investigation period in 20CRv2c (even though non-significant anomalies cover roughly the
260 same area as in 20CRv2c (not shown)). This hints towards decadal variations in the strength
261 of the regression, but could also be due to biases in the reanalyses.

262 To check for such biases we compared all reanalyses with the SLP reconstruction dataset
263 HadSLP2r (**Allen and Ansell 2006**), and found that for the regression analysis using the time
264 period 1901–2010, 20CRv2c overestimates the polar sea level pressure response, whereas
265 ERA20C is much closer to HadSLP2r (See Supplement Figure 6). This would indeed support
266 the notion of decadal variations in the strength of the relationship between predictor and
267 predictand. However, it is worth highlighting that this overestimation for 20CRv2c is not
268 visible for the 1851–2010 period, where the regression anomalies resemble HadSLP2r much
269 closer.

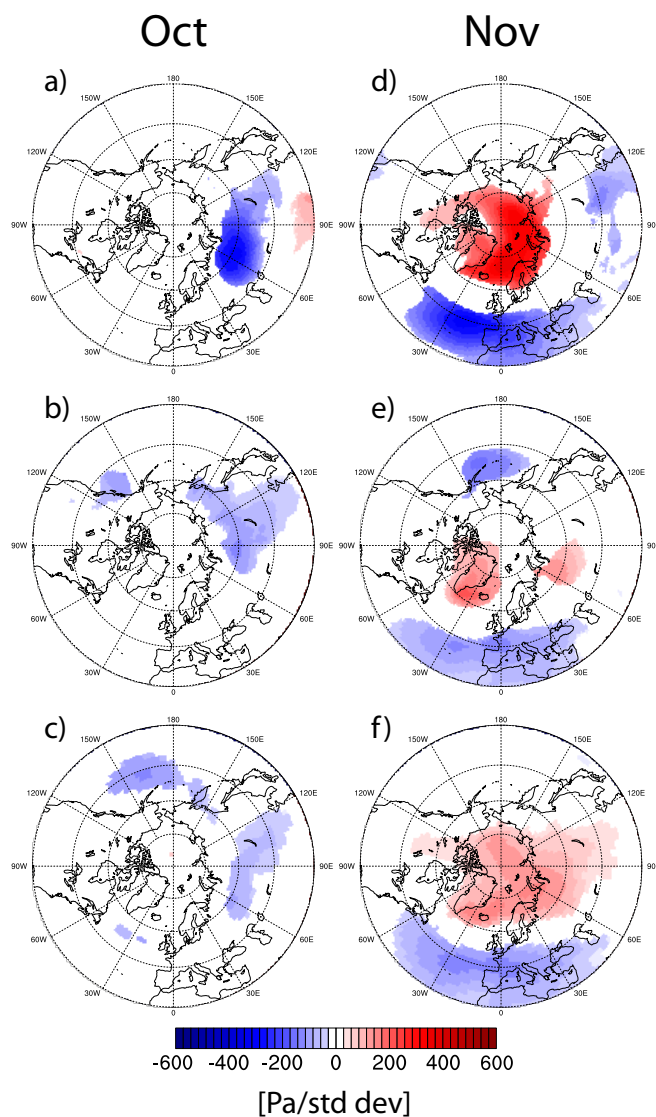


Figure 2: DJF sea level pressure [Pa/std dev] anomalies projected onto snow indices (see Figure 1) for October (left) and November (right) for a and d) MERRA2 covering 1981–2015, b and e) ERA20C covering 1901–2010 and c and f) 20CRv2c covering 1851–2010. Only anomalies >95% significance level are shown.

We investigate other possible predictors for wintertime NAO via regressed anomalies onto the November Barents-Kara-Sea (BKS) ice concentration, November–December mean polar

277 GPH at 10 hPa, October AMO and October ENSO indices (Figure 3). The periods for
278 MERRA2 and ERA20C are identical as for Figure 2, whereas the anomaly plots for 20CRv2c
279 are using the maximum period covered in the reconstructions, namely 1851–2010 in the sea
280 ice reconstruction, 1856–2010 in the AMO reconstruction, 1901–2010 for the polar 10 hPa
281 GPH index taken from ERA20C, and 1870–2010 for the ENSO reconstruction.

282 As can be seen from Figure 3, the 35-year-long analysis in MERRA2 shows November sea
283 ice concentration and early winter stratospheric heights to regress a similar SLP pattern than
284 the November snow index. Positive SLP anomalies over Iceland and Greenland combined
285 with negative anomalies over Southern Europe and the adjacent North Atlantic shape a
286 negative NAO-like pattern in DJF (Figure 3a). On the other hand, the interannual signals in
287 the October AMO and ENSO indices do not point towards such a pressure distribution. The
288 small interannual changes and low frequency of the AMO combined with the short sample
289 period prohibit most of the significance, only Southern Eurasia shows regions with elevated
290 SLP. Anomalies regressed on the ENSO index show, as expected, significance mostly for the
291 North Pacific and North American region.

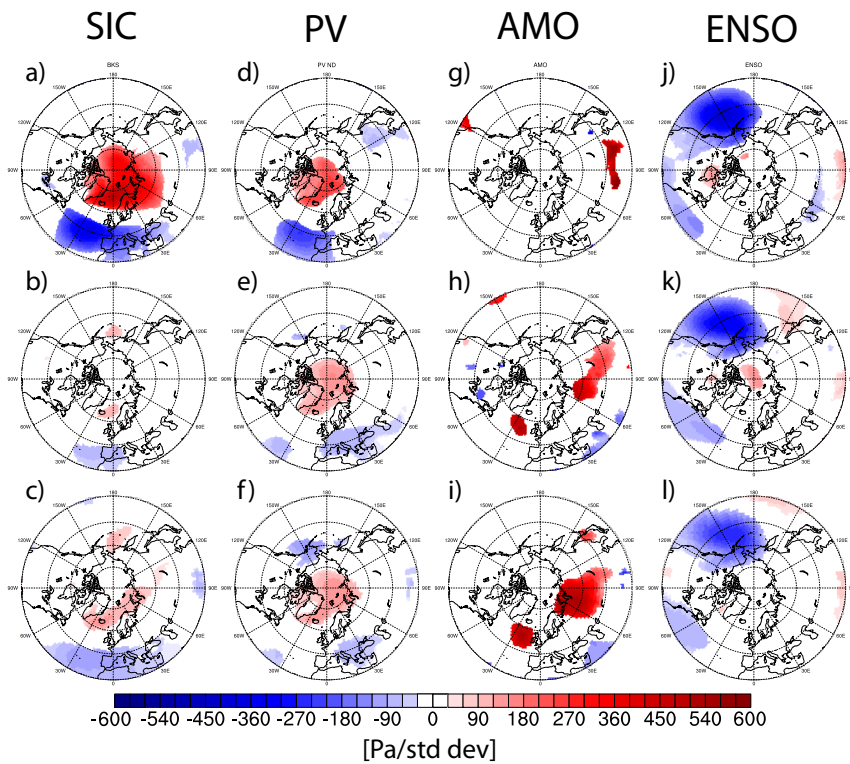
292 Looking at the regression patterns in the centennial reanalyses, the NAO-like pattern in the
293 SLP anomalies regressed onto sea ice and stratospheric GPH can still be seen, however the
294 extent and strength is substantially reduced compared to MERRA2 as well as compared to the
295 regression using November snow as predictor. Again, ERA20C shows a decrease in the
296 significant anomalies regressed onto sea ice compared to 20CRv2c, with possible reasons
297 already discussed above. Elevated geopotential heights at 10 hPa consistently increase polar
298 sea level pressure in the following winter months, however the impact over the European and
299 North Atlantic domain severely decreases in the centennial reanalyses.

300 SLP anomalies regressed onto the AMO index show significant positive SLP regions for large
301 parts of Eurasia as well as positive anomalies over the North Atlantic west of Great Britain.
302 Interesting to note in 20CRv2c is the very strong high-pressure anomaly reaching from the
303 BKS to the southern part of the Ural mountains, a prominent feature often found for years
304 with positive AMO and negative sea ice concentration, frequently linked to a high frequency
305 of Ural blockings (UBs). SLP distribution after El Niño events does not change considerably
306 irrespective of the dataset and time period used. A strong Pacific signal shows the northern
307 part of the Pacific-North American pattern (PNA) with negative SLP anomalies over the
308 eastern North Pacific. Given the autocorrelation in the AMO and BKS sea ice index, the

309 significance in Figure 2abc as well as Figure 2ghi might be severely lower due to the reduced
 310 amount of degrees of freedom.

311

312



313

314 *Figure 3: DJF sea level pressure [Pa/std dev] anomalies projected onto BKS ice concentration in November (far left), polar*
 315 *10 hPa GPH November December mean (left), October AMO (right) and October ENSO indices (far right) for adgi)*
 316 *MERRA2 covering 1981–2015, behk) ERA20C covering 1901–2010 and cfil) 20CRv2c covering 1851–2010. Regression*
 317 *values for BKS ice concentrations were multiplied by minus one to aid comparability. Only anomalies >95% significance*
 318 *level are shown.*

319 To investigate the vertical development of climate anomalies connected with the November
 320 snow dipole, Figure 4 shows the zonal mean anomalies of zonal wind and temperature in
 321 ERA20C projected onto the ERA20C November snow index (for an evaluation with an
 322 upper-air climate reconstruction see Supplementary Figure 7). The temporal evolution of the
 323 anomalies ranging from October to February shows that stratospheric warming occurs

324 simultaneously within the same month as a positive snow cover dipole, with no stratospheric
325 warming leading that development. Instead, significant lower troposphere warming is shown
326 between 60°–90°N for October. The warming signal then dominates the stratosphere and
327 upper troposphere in December, after which the strongest anomalies subside into the lower
328 stratosphere and tropopause in January and February. This development of atmospheric
329 temperatures is mirrored in the evolution of the polar vortex, where a reduction of the polar
330 vortex and strengthening of the subtropical jet is seen together with the emergence of the
331 November snow dipole, after which the region of strongest anomalies migrates from the
332 upper stratosphere to the upper troposphere.

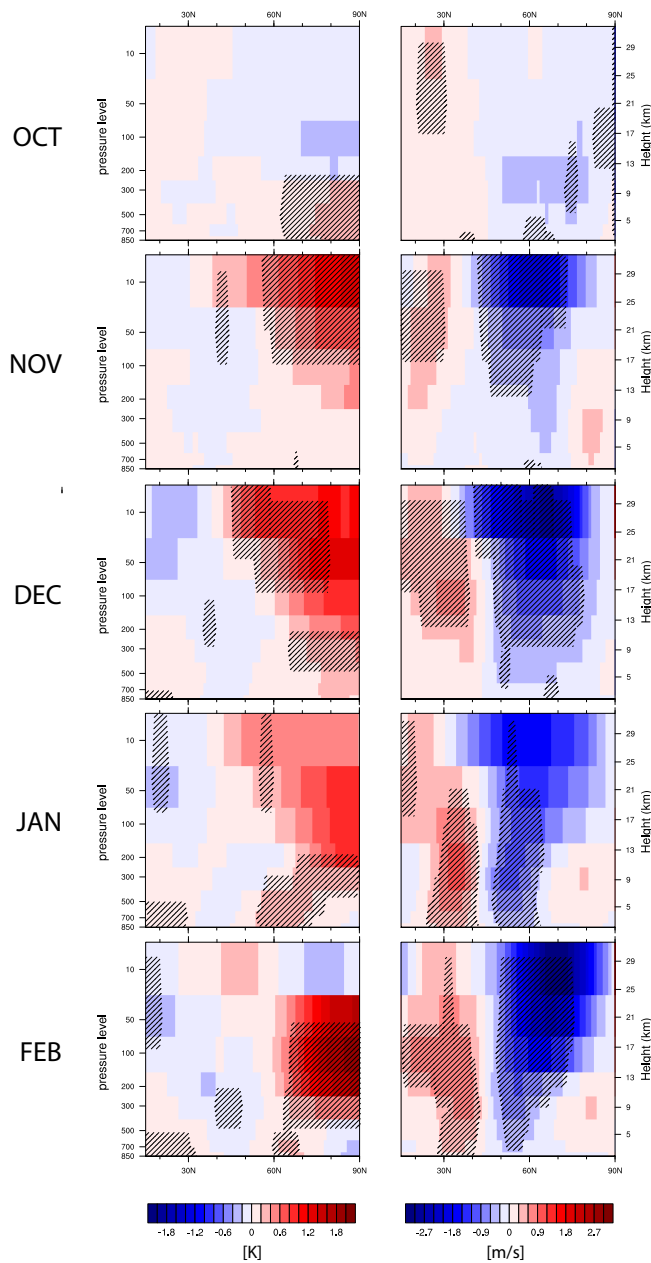


Figure 4: Zonal mean (180°E–180°W, 15°N–90°N) left) temperature anomalies and right) zonal mean zonal wind anomalies projected onto snow indices in November for ERA20C covering 1901–2010. Shading indicates 95% significance level.

336 To address the physical reasons as to how the low sea ice and high snow indices are
337 connected, climate anomalies are regressed onto BKS ice concentrations for November
338 (Figure 5). Compared to factors such as AMO and ENSO, BKS sea ice shows a distinct snow
339 cover dipole coinciding with a high-pressure anomaly over the BKS and the northern Ural
340 mountains, which supports a regional atmospheric blocking and cold air advection on its
341 eastern flank. This cold air anomaly supports increased snow cover over eastern Eurasia,
342 while relatively warm temperatures reduce the snow cover over eastern Europe. It should be
343 noted that October BKS ice concentration shows qualitatively the same pattern for November
344 snow cover anomalies (not shown), however not statistically significant.

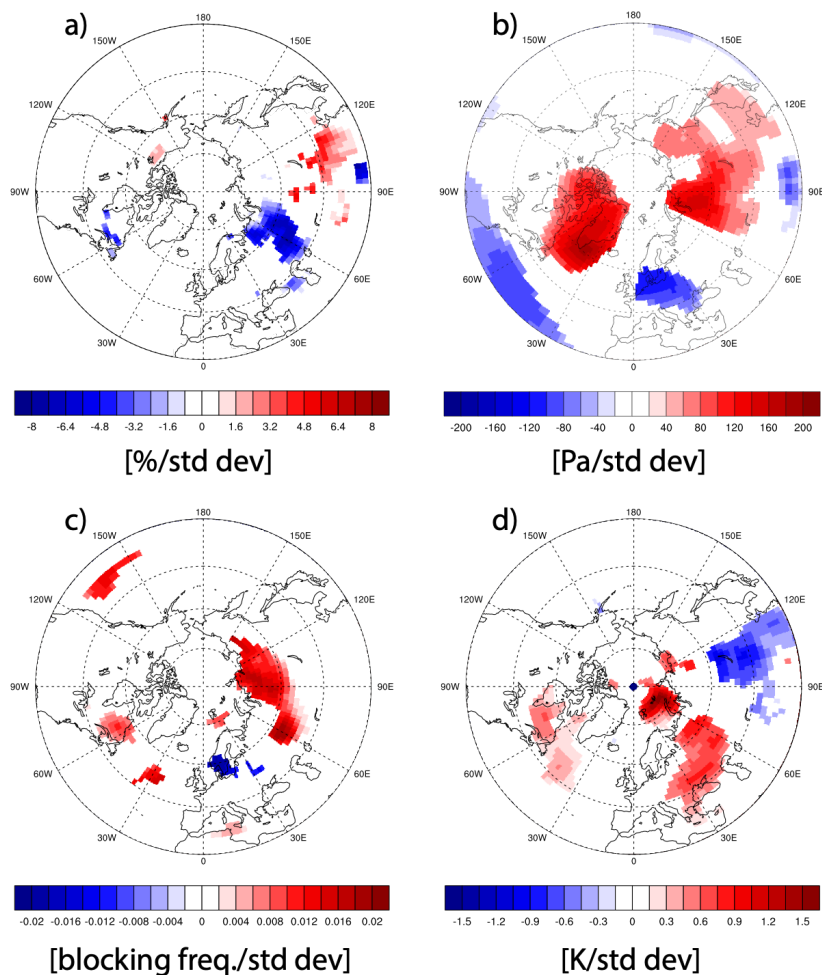


Figure 5: 20CRv2c November anomalies projected onto BKS ice concentration in November covering 1851–2010. Regression values for BKS ice concentrations were multiplied by minus one to aid comparability. a) November snow cover [%/std dev] anomalies projected onto BKS ice concentration in November, b) November SLP [Pa/std dev] anomalies projected onto BKS ice concentration in November, c) November atmospheric blocking [blocking per season/std dev] anomalies projected onto BKS ice concentration in November and d) November 2m temperature [K/std dev] anomalies projected onto BKS ice concentration in November. Only anomalies >95% significance level are shown.

Formatted: Normal, Left

Formatted: Font colour: Auto, German

b. Interdecadal links

The interdecadal evolution of the November snow index is shown in Figure 6. 21-year running means of the normalized time series of AMO, BKS ice and snow hint towards a multidecadal frequency, similar in wave length to the AMO and BKS ice anomalies. Even though we refrain from correlating these time series due to the the 21-year filter (Trenary and DelSole, 2016), we find the possible mechanism behind the decadal co-occurrence of warm North Atlantic SSTs, reduced sea-ice and increased snow cover gradient to be physically plausible (Luo et al. 2017). As Luo et al. (2017) point out, warm North Atlantic water reduces the BKS ice concentration, which decreases the meridional temperature gradient and strong westerly winds, which in turn supports high pressure over the Ural mountains and with that, cold air advection towards eastern Eurasia. It should be noted however, that the AMO and the November snow index are out-of-phase between 1880 and 1920, where uncertainties in both products are largest.

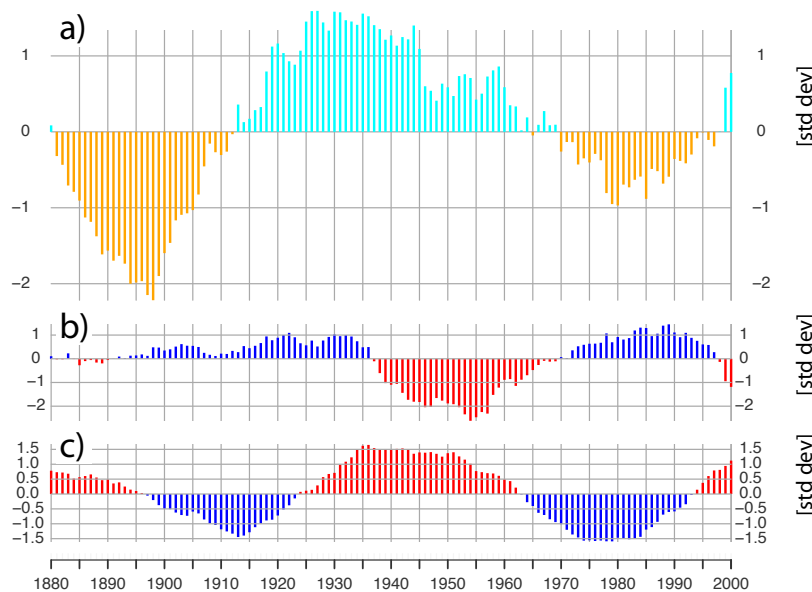
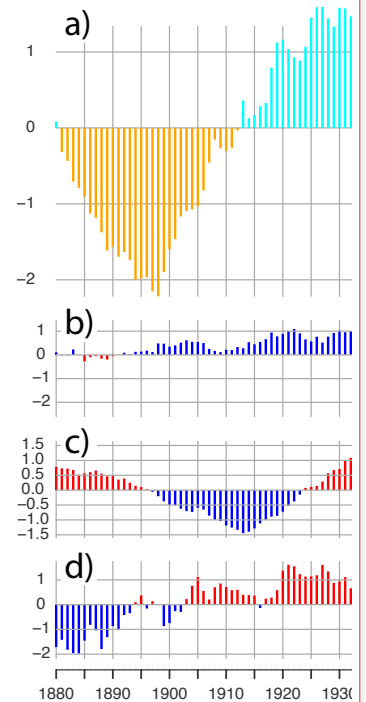


Figure 6: 21-year running means of a) November snow index from 20CRv2c, b) November BKS ice concentration, c) October AMO.

The more critical question is the interdecadal evolution of the relationship between the predictor and the predictand. Similar to Peings et al. (2013) and Douville et al. (2017), we

Deleted: ENSO,



Deleted:

Deleted: and d) October ENSO reconstruction.

377 apply a 21-year running correlation covering the period 1901–2010 to examine the
378 stationarity of the relationship and differences between 20CRv2c and ERA20C.

379 Figure 7 summarizes the correlation over time for multiple pairs of climate variables. As
380 Figure 7b points out, the sign of the November snow to winter NAO relationship in 20CRv2c
381 is negative throughout the whole 20th century. Periods with negative correlations can be found
382 at the beginning and the end of the century, with relatively weak correlation during the 1930s
383 and 1970s. The periods of strong negative correlations overlap with commonly known Arctic
384 warming periods, the early 20th-century Arctic warming (ETCAW) and the ongoing recent
385 Arctic warming in context of anthropogenic global warming. In ERA20C, these periods are
386 actually marked by positive correlations, indicating a non-stationary relationship between
387 these two variables. Even stronger decadal variability can be seen for the running correlations
388 between the October snow index and winter NAO-like ~~signal~~ (Figure 7a), with periods of
389 pronounced negative correlations during the early 20th century Arctic warming and the 1980s.
390 Emerging since the 1970s is a negative relationship shown in Figure 7e between BKS ice
391 reduction (multiplied by minus one to aid comparability) and the formation of a negative
392 NAO signal in the following winter, with very weak negative correlations for the ETCAW.

393 Together with the emergence of the sea ice to NAO relationship, negative correlations
394 between BKS sea ice and November snow index (Figure 7d) as well as between stratospheric
395 warming and winter NAO strengthen towards the end of the 20th century (Figure 7f). This
396 strengthening is also found in ERA20C for the correlation between November snow and a
397 following stratospheric warming, where 20CRv2c shows consistently positive correlation
398 values throughout the 20th century (Figure 7c).

399 Overall, the 20CRv2c November snow index shows a more stationary relationship with
400 tropospheric and stratospheric winter circulation than ERA20C. Possible explanations for this
401 behavior will be discussed in the following section.

402 For all of the linear relationships shown in Figure 7 we performed a Durbin-Watson test to
403 check for serial correlation between two variables and did not find any compelling indication
404 for co-dependence in any case (see Supplementary Table 1). Moreover, we investigated
405 different running correlation windows (11 years, 21 years, 25 years, and 31 years) and find
406 that the main outcome of the analysis is not dependent on the choice of the correlation
407 window (see Supplementary Figure 8).

Deleted: impact

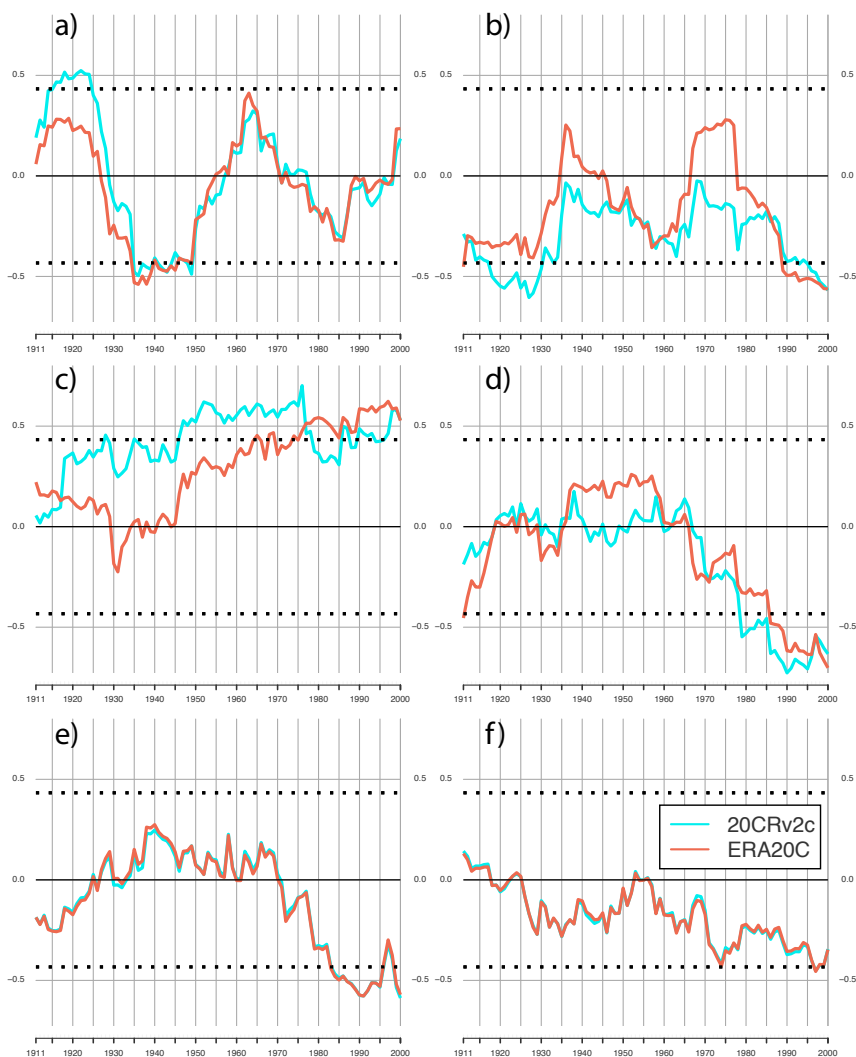


Figure 7: 21-year centered running correlation time series between a) October snow index and DJF NAO, b) November snow index and DJF NAO, c) November snow index and mean November-December polar 10 hPa GPH index, d) November snow index and November BKS ice concentration, e) November BKS ice concentration multiplied by minus one to aid comparability and DJF NAO and f) mean November-December polar 10 hPa GPH and DJF NAO index. Black dashed line indicating the 95% confidence level for a two-sided student's T-test assuming independence and normal distribution.

Based on the results from Figure 7 (and the overall significance of linear relationships, see Supplementary Figure 9) we investigate very basic linear multiple and simple regression

models to predict the upcoming DJF NAO index sign and assess the contributions to the prediction skill by November sea ice, November snow cover and November December mean stratospheric conditions. For the period 1901–2010 we investigate three different multiple regression models with

$$\text{a) DJF NAO}(t) = a_1 \times \text{Nov. snow cover}(t) + b_1 \times \text{Nov. BKS sea ice}(t) + c_1 \times \text{ND 10hPa GPH}(t)$$

$$\text{b) DJF NAO}(t) = a_1 \times \text{Nov. snow cover}(t) + b_1 \times \text{Nov. BKS sea ice}(t)$$

$$\text{c) DJF NAO}(t) = a_1 \times \text{Nov. snow cover}(t) + b_1 \times \text{ND 10hPa GPH}(t)$$

and one simple linear regression model

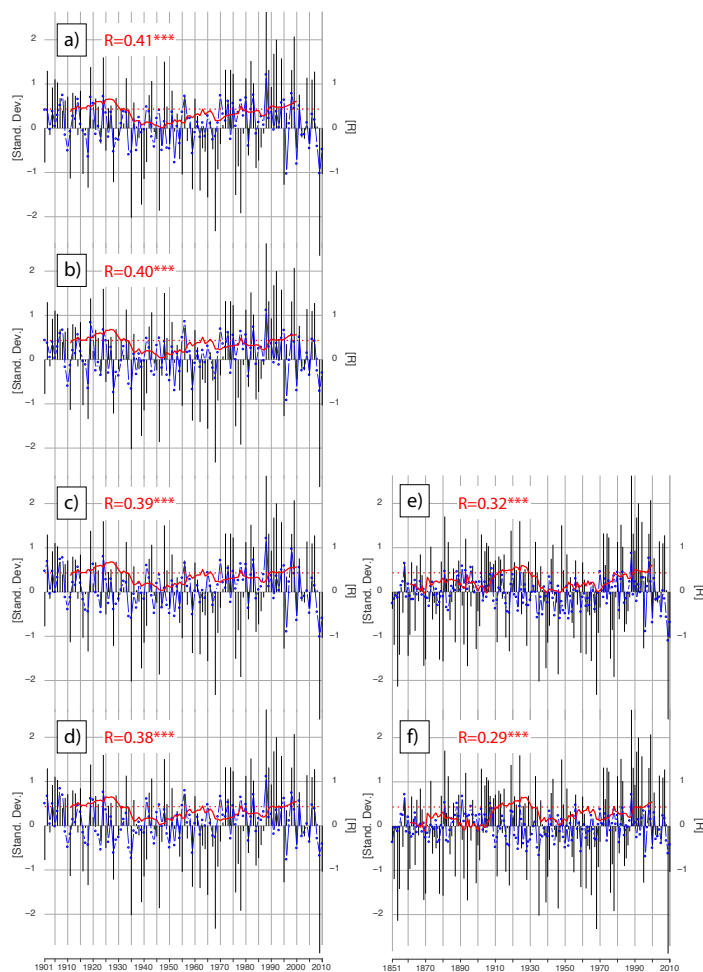
$$\text{d) DJF NAO}(t) = a_1 \times \text{Nov. snow cover}(t)$$

where DJF NAO is the standardized NAO index calculated by EOF analysis of 20CRv2c SLP data, Nov. snow cover is the November 20CRv2c snow cover index, Nov. BKS sea ice is the Walsh et al. November BKS sea ice index and ND 10hPa GPH is the ERA20C November December mean 10hPa GPH index with a_1, b_1, c_1 being the constants determined by the least-squares calculations. Moreover, we perform b) and d) also for the period 1851–2010.

Figure 8 shows original and predicted normalized DJF NAO values together with the 21-year running correlation of both indices. Overall correlation values are low but significant for the 110-year time period (ranging from 0.41 to 0.38) but specific periods of high correlation emerge for both Arctic warm periods, the first one being centered around 1925 and the second one being centered around the year 2000 with both periods reaching correlation coefficients above 0.6. The multiple regression prediction model with three different predictors performs best, with a significant correlation to the original NAO variability of 0.41 for 110 years (Figure 8a). Nevertheless, November snow cover seems to add most of the prediction skill, since the decrease in correlation coefficient between the multiple regression model with three predictors and the simple linear regression model with just November snow cover as a predictor is 0.03. Moreover, periods of high correlation coefficients align with periods of strong negative relationships in Figure 7b.

For the same empirical prediction model using 160 years, the overall correlation coefficients decrease to around 0.3. As expected, the same periods of increased prediction skill emerge

446 (Figure 8e&f) and the added prediction skill of sea ice is low. It should be noted however, that
 447 sea ice increases prediction skill during the current Arctic warming period, as well as the end
 448 of the 19th century with 2nd highest correlation coefficients centered around 1890 (not shown).



449

450 *Figure 8: Comparison of 1901–2010 20CRv2c DJF standardized NAO values based on EOF analysis with predicted values*
 451 *from multiple and simple linear regression models showing a) multiple linear regression model with November snow cover*
 452 *index, November BKS sea ice index and ND 10hPa geopotential height index with an overall correlation of 0.41, b) multiple*
 453 *linear regression model with November snow cover index and ND 10hPa geopotential height index with an overall*
 454 *correlation of 0.4, c) multiple linear regression model with November snow cover index and November BKS sea ice index*
 455 *with an overall correlation of 0.39, d) simple linear regression model with November snow cover index and November BKS*

456 sea ice index with an overall correlation of 0.38. e) and f) same as c) and d) but for the period 1851–2010 respectively. Left
457 Y-axis indicates standard deviation, right Y-axis indicates correlation coefficient. Red dashed line indicates 95% significance
458 level for a 21-year period.

459

460 4. Discussion

461 We used a variety of reanalyses and reconstructions to address some of the open questions
462 regarding the relationship between Eurasian snow cover and the state of the NAO in the
463 following winter.

464 Given the highly discussed research topic of Northern Hemisphere sea ice cover and snow
465 cover impact on mid-latitude circulation (Cohen et al., 2019), as well as the highlighted need
466 to investigate relationships over several decades (Kolstad and Screen 2019), we investigated
467 a promising November west-east snow cover dipole over Eurasia (Gastineau et al., (2017);
468 Han and Sun (2018)) and its relationship to the DJF NAO state up to the middle of the 19th
469 century to cover 150 years of internal and external climate forcings. Given the importance for
470 seasonal prediction, we addressed the question of stationarity of said relationship as well as its
471 context within other common Northern Hemispheric predictors.

472 Compared to Gastineau et al. (2017) and Han and Sun (2018), we could extend the
473 reanalysis study period from 35 to 150 years and highlighted the consistently negative sign of
474 the snow-NAO relationship in the 20CRv2c dataset. Partial correlations for 110 years show
475 that reduced BKS sea ice shows a similar response in DJF SLP anomalies, however its
476 statistical importance, and therefore quality as being the prime predictor, is less than the
477 November snow index (see Supplementary Table 2 for partial correlations). This is also found
478 in simple multiple regression prediction models, where the November snow cover index was
479 incorporating the major share of the prediction power. Extending the analysis of Gastineau et
480 al. (2017) to 150 years further underlines the lack of snow–atmosphere feedback in most of
481 the CMIP5 models and reduces the probability that the snow-NAO link is due to random
482 internal variability at the end of the 20th century.

483 Moreover, given the monthly development of vertical temperature anomalies related to a high
484 snow cover index supports the theoretical framework (Cohen et al., 2014; Henderson et al.
485 2018) for a Eurasian snow cover to stratosphere link in reanalyses for at least the 20th century
486 and probably beyond. We found surface cooling and snow cover expansion east of the sea ice

Deleted: can

Deleted: find

Deleted: a

490 anomaly, where cold air is advected on the eastern side of a Ural blocking anomaly (Figure
491 5). The increased geopotential heights and the related Rossby-Wave energy reach the
492 stratosphere (Supplementary Figure 7), where a stratospheric warming and a slow down of
493 the Polar Vortex manifests (Figure 4). These anomalies reach the troposphere in January and
494 February where they express themselves as a negative NAO signal (Figure 2). It is
495 noteworthy, that all of these features are significantly correlated with the November snow
496 cover index for more than 100 years.

497 **Peings et al. (2013)** and the follow up study by **Douville et al. (2017)** found that the October
498 and October–November mean snow cover over a broader region of Northern Eurasia, and its
499 relationship to the wintertime NAO is indeed not stationary over time. We **found** a strong
500 relationship between the reduced variance of the snow index time series with the reduction in
501 correlation strength of snow cover and the wintertime NAO (Figure 9). The reduction of
502 variance is even stronger in ERA20C than in 20CRv2c, which would explain the less
503 stationary correlations in ERA20C. Furthermore, such periods of low snow variability
504 coincide with a reduction of polar vortex variability, hinting even more so towards possible
505 links between November snow and stratospheric temperatures in the following month.
506 Together with the snow cover index, the November BKS sea ice index shows increased
507 variability with strengthened negative correlation to DJF NAO during at the end of the 20th
508 century (see Supplementary Figure 11).

509 These periods of increased variability in the November snow cover index co-occur arguably
510 with the common Arctic warming periods of the 20th century, the ETCAW (**Wegmann et al.,**
511 **2016; Hegerl et al., 2018**) and the recent ongoing Arctic warming with peak variance and
512 correlation values centered around the years 1920 and 2000. Interestingly, October snow
513 cover index and BKS sea ice index variability peaks slightly after the ETCAW around the
514 year 1945. Analysing temperature anomalies (not shown) for all three periods reveals more
515 continental warming over Russia for the period 1911-1930 whereas warming between 1936-
516 1955 is located very much at the Kara Sea coast of Russia. **Both**, the October snow index and
517 the BKS sea ice index, are **thus** impacted by **the locally increased near-surface temperatures**
518 **during the latter period**. Generally, Arctic warming periods appear to increase variability of
519 cryospheric predictors considerably and thus strengthen their **value** in seasonal prediction
520 frameworks. Given the importance of stratospheric variability for seasonal prediction and the
521 apparent relationship between snow cover variability and stratospheric variability (Figure 9),
522 it can be expected that the cryosphere-stratosphere pathway is also considerably stronger in

Deleted: find

Deleted: , where

Deleted: b

Deleted: impact

527 Arctic warm periods than for cold periods. Moreover, in our statistical analysis, we found no
528 indication for a stratospheric precursor of November snow cover anomalies.

529 In accordance to the shorter time frame analysis of **Sun et al. (2019)**, decadal variability of
530 the November snow cover index seems mostly dominated by low-frequency variability in the
531 AMO and subsequently reduced or increased polar sea ice concentration. This mechanism is
532 also supported by the results of **Luo et al. (2017)**, who highlighted the decadal relationship
533 between a positive AMO, reduced sea ice and increased Ural blocking for the second half of
534 the 20th century. Looking at this mechanism on an interannual basis, we showed a robust
535 strengthening of the November snow dipole with decreasing BKS ice concentration,
536 circulation changes over the BKS region and consequently cold air advection towards the
537 eastern part of the snow dipole region for a period of 150 years. With this, our results support
538 recent studies, which point out the counterintuitive mechanism of Arctic warming and
539 increased continental snow cover via sea ice reduction and circulation changes (**Cohen et al.,**
540 **2014; Wegmann et al., 2015; Yeo et al., 2016; Gastineau et al., 2017**).

541 **Peings (2019)** performed model experiments with nudged November Ural blocking fields,
542 BKS ice and snow anomalies. The author found that UB events are not triggered by reduced
543 sea ice, but in fact lead sea ice decrease. Moreover, more November snow alone did not lead
544 to an increase in blocking frequency, nor to a stratospheric warming. The study highlights the
545 UB events as primary predictor for a negative NAO and the Warm Arctic-cold Continents
546 (WACC) pattern. On the other hand, **Luo et al. (2019)** established a causal chain via a
547 stratospheric pathway from reduced sea ice to reduced potential vorticity gradient and
548 increased blocking events leading to cold extremes over Eurasia. We computed the field
549 average of blocking frequency within the domain of **Peings (2019)** (10°W-80°E, 45-80°N)
550 and could find a strong correlation with the WACC pattern over time, however only for DJF
551 blocking events (not shown).

552 We found a correlation of November UB events with wintertime NAO, which however is still
553 weaker than the relationship with the November snow dipole, as well as our BKS ice index
554 (see Supplementary Figure 10). Moreover, blockings within the domain of **Peings (2019)**
555 (10°W-80°E, 45-80°N) are not related to a snow dipole whatsoever, neither in October nor in
556 November (see Supplementary Figure 10). That said, we want to highlight the fact that the
557 blocking pattern emerging in Figure 5 is mostly outside of the boundaries of this UB index
558 (10°W-80°E, 45-80°N), and thus might not be caught by this recent study. Furthermore,
559 **Peings (2019)** applies a very general snow cover increase in his nudging experiment, rather

Deleted: is

561 than a snow dipole with a west to east gradient. Finally, although we focused here on the
562 connection to the NAO, we did not find strong significant correlations between autumn snow
563 and winter WACC. As pointed out by **Peings (2019)**, the most important driver for the
564 WACC signal is the Ural blocking, for which we found strong correlations throughout the 20th
565 century (not shown).

Deleted: ind

566 Overall, we advocate the importance of the signal-to-noise ratio rather than mean states for
567 the evolution of the November snow to winter NAO relationship. In our statistical analysis,
568 we did not find any indication for a centennial relationship between the autumn ENSO or
569 autumn QBO sign with the variability of the relationship between November snow cover and
570 DJF NAO (not shown). As mentioned above, we found the strongest influence to be the
571 increased variability of the system due to energy uptake.

Deleted: ,

572 That said, a source of uncertainty is the disagreement between ERA20C and 20CRv2c when it
573 comes to the stationarity of the relationship. 20CRv2c shows negative correlation throughout
574 the whole 20th century, whereas ERA20C flips the sign of the correlation in the late 1930s and
575 late 1970s. The same relationship but using October snow shows high agreement between the
576 two datasets, which is the same case for the correlations between snow and stratospheric
577 GPH. We therefore conclude, that the information stored in the November snow cover in
578 20CRv2c is slightly different to the information stored in the ERA20C snow depth.
579 **Wegmann et al. (2017)** found that Eurasian November snow depth shows much larger
580 disagreement between 20CRv2c and ERA20C than the same snow depth in October. In the
581 same study, the authors found decadal trends (although linear trend subtraction for all
582 predictor time series was done for this study) in ERA20C snow depth which might impact the
583 running correlations. Finally, since snow depths are relatively low in October, differences
584 between using snow cover and snow depth might be less important from an energy transfer
585 point of view.

586 The disagreement between ERA20C and 20CRv2c may also be related to uncertainties and
587 inhomogeneities in both reanalyses. Many studies showed that both ERA20C and 20CRv2c
588 are not suitable for studies looking at trends (e.g. **Brönnimann et al., 2012; Krüger et al.,**
589 **2013**) and may include radical shifts in atmospheric circulation, particularly over the Arctic
590 (e.g. **Dell'Aquila et al., 2016; Rohrer et al., 2019**). However, **Rohrer et al. (2019)** showed
591 that although trends in centennial reanalyses may be spurious, at least in the Northern
592 Hemisphere year-to-year variability of mid-tropospheric circulation is in agreement even in
593 the early 20th century.

Formatted: Don't keep with next

Deleted: ¶

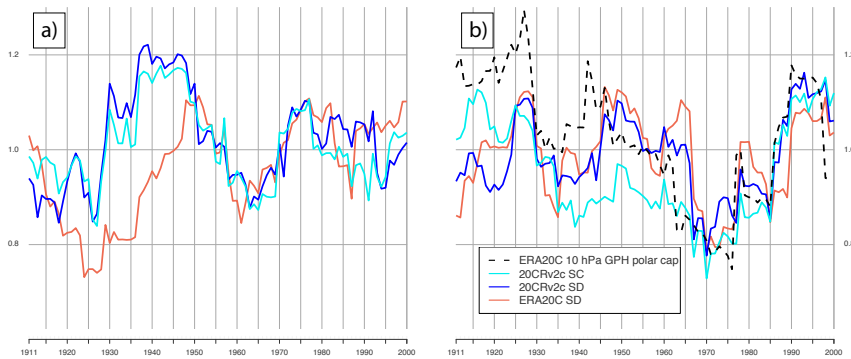


Figure 9: 21-year running standard deviation time series of a) October snow index and b) November snow index in ERA20C and 20CRv2c (snow cover and snow depth). Dashed black line shows running standard deviation of 10 hPa November December mean GPH over the polar regions.

5. Conclusion

Several reconstruction and reanalysis datasets were used to examine the link between autumn snow cover, ocean surface conditions and the NAO pattern in winter for the whole 20th century and into the 19th century. We found evidence for a manifestation of a negative NAO signal after November with a strong west-to-east snow cover gradient, with this relationship being significant for the last 150 years. Interdecadal variability for this relationship seems to be linked to Arctic warm periods which increase the variability of the cryospheric predictors considerably. As a result, increased variability in the predictors helps to generate a better seasonal prediction estimation.

Furthermore, our analysis of centennial time series supports studies pointing out ~~the link of~~ autumn snow ~~to~~ stratospheric circulation as well as the ~~co-occurrence~~ between reduced BKS ice concentration and increased snow cover in eastern Eurasia. The latter mechanism is triggered via the development of an atmospheric high-pressure anomaly adjacent to the BKS sea ice anomaly, which transports moisture and cold air along its eastern flank into the continent. The interdecadal evolution of the November snow index also points towards ~~co-~~dependence with high North Atlantic SSTs subsequently reduced sea ice.

Extending the investigation period from 35 to 110 and up to 150 years increases the confidence in recently proposed physical mechanisms behind cryospheric drivers of atmospheric variability and decreases the probability of random co-variability between the Arctic cryosphere changes and mid-latitude climate.

Deleted: the impact

Deleted: on

Deleted: connection

Deleted: a

625 For future studies regarding seasonal prediction, we emphasize the use of the November snow
626 dipole concerning a forecasting of the winter NAO state. Nevertheless, periods of weak
627 correlation might occur again, especially since it is uncertain how the sea ice to snow
628 relationship will change with stronger anthropogenic global warming, once the Arctic is ice
629 free in summer or the local warming is strong enough to override the counterintuitive snow
630 cover increase. Thus, further studies are needed to investigate the interplay between Arctic
631 sea ice and continental snow distribution. Future experiments should take into account year-
632 to-year variability and realistic distribution of snow cover if links to the stratosphere are to be
633 examined.

634

635 **Acknowledgements**

636 Marco Rohrer was supported by the Swiss National Science Foundation under Grant 143219.
637 The Twentieth Century Reanalysis Project datasets are supported by the U.S. Department of
638 Energy, Office of Science Innovative and Novel Computational Impact on Theory and
639 Experiment (DOE INCITE) program, and Office of Biological and Environmental Research
640 (BER), and by the National Oceanic and Atmospheric Administration Climate Program
641 Office. The ECMWF 20th Century Reanalyses and model simulations are supported by the
642 EU FP7 project ERA-CLIM2. We thank Morgan Gray for editorial support.

643 **Data Availability**

644 The MERRA2 reanalysis data is publicly available at the NASA EARTHDATA repository
645 (<https://disc.gsfc.nasa.gov/daac-bin/FTPSubset2.pl>). The ERA-20C reanalysis data is publicly
646 available at the ECMWF data repository (<https://apps.ecmwf.int/datasets/>). The 20CRv2c
647 reanalysis data is publicly available at the NOAA Earth System Research Laboratory
648 repository (https://www.esrl.noaa.gov/psd/data/gridded/data.20thC_ReanV2c.html). The
649 blocking algorithm is publicly available at <https://github.com/marco-rohrer/TM2D>. The AMO
650 reconstruction data is a publicly available at the NOAA Earth System Research Laboratory
651 (<https://www.esrl.noaa.gov/psd/data/timeseries/AMO/>). The Niño 3.4 reconstruction is
652 publicly available at the GCOS Working Group on Surface Pressure repository
653 (https://www.esrl.noaa.gov/psd/gcos_wgsp/Timeseries/Nino34/). The NAO reconstruction is
654 publicly available at the Climate Research Unit repository
655 (<https://crdata.uea.ac.uk/cru/data/nao/>). The Walsh et al. sea ice concentration reconstruction

656 is publicly available at the National Snow and Ice Data Center repository
657 (<https://nsidc.org/data/g10010>).

658 **Author Contribution**

659 M.W. devised the study, the main conceptual ideas and the proof outline. M.R. assisted with
660 data availability and performed the blocking algorithm. M.W. wrote the manuscript in
661 consultation with M.S.-O. and G.L., who aided in interpreting the results.

662 **Competing interest**

663 The authors declare that they have no conflict of interest.

664 **References**

- 665 Allan, R., and T. Ansell, 2006: A New Globally Complete Monthly Historical Gridded Mean
666 Sea Level Pressure Dataset (HadSLP2): 1850-2004. *J. Climate*, 19, 5816-5842.
- 667 Athanasiadis, P. J., Bellucci, A., Scaife, A. A., Hermanson, L., Materia, S., Sanna, A., ... and
668 Gualdi, S. (2017). A multisystem view of wintertime NAO seasonal
669 predictions. *Journal of Climate*, 30(4), 1461-1475.
- 670 Belleflamme A, Fettweis X, Erpicum M (2015) Recent summer Arctic atmospheric
671 circulation anomalies in a historical perspective. *Cryosphere* 9:53–64
- 672 Blackport, Russell, and James A. Screen. "Influence of Arctic Sea Ice Loss in Autumn
673 Compared to That in Winter on the Atmospheric Circulation." *Geophysical Research*
674 *Letters* 46.4 (2019): 2213-2221.
- 675 Blackport, R., Screen, J.A., van der Weil, K., and Bintanja, R. (2019). Minimal influence of
676 reduced Arctic sea ice on coincident cold winters in mid-latitudes. *Nature Climate*
677 *Change*, ?
- 678 Boland, E. J., Bracegirdle, T. J., and Shuckburgh, E. F. (2017). Assessment of sea ice-
679 atmosphere links in CMIP5 models. *Climate Dynamics*, 49(1-2), 683-702.
- 680 Brönnimann, S., Luterbacher, J., Staehelin, J., Svendby, T. M., Hansen, G., and Svenøe, T.
681 (2004). Extreme climate of the global troposphere and stratosphere in 1940–42 related
682 to El Niño. *Nature*, 431(7011), 971.

683 Brönnimann, S., Xoplaki, E., Casty, C., Pauling, A., and Luterbacher, J. (2007). ENSO
684 influence on Europe during the last centuries. *Climate Dynamics*, 28(2-3), 181-197.

685 Cohen, J., and Entekhabi, D. (1999). Eurasian snow cover variability and Northern
686 Hemisphere climate predictability. *Geophysical Research Letters*, 26(3), 345-348.

687 Cohen, J., Barlow, M., Kushner, P. J., and Saito, K. (2007). Stratosphere–troposphere
688 coupling and links with Eurasian land surface variability. *Journal of Climate*, 20(21),
689 5335-5343.

690 Cohen, J., Screen, J. A., Furtado, J. C., Barlow, M., Whittleston, D., Coumou, D., ... and
691 Jones, J. (2014). Recent Arctic amplification and extreme mid-latitude weather. *Nature*
692 *geoscience*, 7(9), 627.

693 Cohen, J. (2016). An observational analysis: Tropical relative to Arctic influence on
694 midlatitude weather in the era of Arctic amplification. *Geophysical Research*
695 *Letters*, 43(10), 5287-5294.

696 Cohen, J., Pfeiffer, K., and Francis, J. A. (2018). Warm Arctic episodes linked with increased
697 frequency of extreme winter weather in the United States. *Nature communications*, 9(1),
698 869.

699 Cohen, J., Zhang, X., Francis, J., Jung, T., Kwok, R., Overland, J., ... and Feldstein, S. (2019).
700 Divergent consensus on Arctic amplification influence on midlatitude severe winter
701 weather. *Nature Climate Change*, 1-10.

702 Collow, T. W., Wang, W., Kumar, A., and Zhang, J. (2017). How well can the observed
703 Arctic sea ice summer retreat and winter advance be represented in the NCEP Climate
704 Forecast System version 2?. *Climate Dynamics*, 49(5-6), 1651-1663.

705 Cram, T. A., Compo, G. P., Yin, X., Allan, R. J., McColl, C., Vose, R. S., ... and
706 Bessemoulin, P. (2015). The international surface pressure databank version
707 2. *Geoscience Data Journal*, 2(1), 31-46.

708 Crasemann, B., Handorf, D., Jaiser, R., Dethloff, K., Nakamura, T., Ukita, J., and Yamazaki,
709 K. (2017). Can preferred atmospheric circulation patterns over the North-Atlantic-
710 Eurasian region be associated with arctic sea ice loss?. *Polar Science*, 14, 9-20.

711 Dell'Aquila, A., Corti, S., Weisheimer, A., Hersbach, H., Peubey, C., Poli, P., ... and
712 Simmons, A. (2016). Benchmarking Northern Hemisphere midlatitude atmospheric

synoptic variability in centennial reanalysis and numerical simulations. *Geophysical Research Letters*, 43(10), 5442-5449.

Deser, C., Hurrell, J. W., and Phillips, A. S. (2017). The role of the North Atlantic Oscillation in European climate projections. *Climate dynamics*, 49(9-10), 3141-3157

Domeisen, D. I., Garfinkel, C. I., and Butler, A. H. (2019). The teleconnection of El Niño Southern Oscillation to the stratosphere. *Reviews of Geophysics*.

Douville, H., Peings, Y., and Saint-Martin, D. (2017). Snow-(N) AO relationship revisited over the whole twentieth century. *Geophysical Research Letters*, 44(1), 569-577.

Dunstone, N., Smith, D., Scaife, A., Hermanson, L., Eade, R., Robinson, N., ... and Knight, J. (2016). Skilful predictions of the winter North Atlantic Oscillation one year ahead. *Nature Geoscience*, 9(11), 809.

Enfield, D. B., Mestas-Núñez, A. M., and Trimble, P. J. (2001). The Atlantic multidecadal oscillation and its relation to rainfall and river flows in the continental US. *Geophysical Research Letters*, 28(10), 2077-2080.

Francis, J. A. (2017). Why are Arctic linkages to extreme weather still up in the air?. *Bulletin of the American Meteorological Society*, 98(12), 2551-2557.

Furtado, J. C., Cohen, J. L., Butler, A. H., Riddle, E. E., and Kumar, A. (2015). Eurasian snow cover variability and links to winter climate in the CMIP5 models. *Climate dynamics*, 45(9-10), 2591-2605.

Furtado, J. C., Cohen, J. L., and Tziperman, E. (2016). The combined influences of autumnal snow and sea ice on Northern Hemisphere winters. *Geophysical Research Letters*, 43(7), 3478-3485.

García-Serrano, J., Frankignoul, C., Gastineau, G., and De La Cámara, A. (2015). On the predictability of the winter Euro-Atlantic climate: lagged influence of autumn Arctic sea ice. *Journal of Climate*, 28(13), 5195-5216.

Garfinkel, C. I., Schwartz, C., Domeisen, D. I., Son, S. W., Butler, A. H., and White, I. P. (2018). Extratropical Atmospheric Predictability From the Quasi-Biennial Oscillation in Subseasonal Forecast Models. *Journal of Geophysical Research: Atmospheres*, 123(15), 7855-7866.

742 Gastineau, G., García-Serrano, J., and Frankignoul, C. (2017). The influence of autumnal
743 Eurasian snow cover on climate and its link with Arctic sea ice cover. *Journal of*
744 *Climate*, 30(19), 7599-7619.

745 Gelaro, R., McCarty, W., Suárez, M. J., Todling, R., Molod, A., Takacs, L., ... and Wargan,
746 K. (2017). The modern-era retrospective analysis for research and applications, version
747 2 (MERRA-2). *Journal of Climate*, 30(14), 5419-5454.

748 Ghatak, D., Frei, A., Gong, G., Stroeve, J., and Robinson, D. (2010). On the emergence of an
749 Arctic amplification signal in terrestrial Arctic snow extent. *Journal of Geophysical*
750 *Research: Atmospheres*, 115(D24).

751 Han, S., and Sun, J. (2018). Impacts of Autumnal Eurasian Snow Cover on Predominant
752 Modes of Boreal Winter Surface Air Temperature Over Eurasia. *Journal of Geophysical*
753 *Research: Atmospheres*, 123(18), 10-076.

754 Handorf, D., Jaiser, R., Dethloff, K., Rinke, A., and Cohen, J. (2015). Impacts of Arctic sea
755 ice and continental snow cover changes on atmospheric winter
756 teleconnections. *Geophysical Research Letters*, 42(7), 2367-2377.

757 Hegerl, G. C., Brönnimann, S., Schurer, A., and Cowan, T. (2018). The early 20th century
758 warming: anomalies, causes, and consequences. *Wiley Interdisciplinary Reviews:*
759 *Climate Change*, 9(4), e522.

760 Henderson, G. R., Peings, Y., Furtado, J. C., and Kushner, P. J. (2018). Snow-atmosphere
761 coupling in the Northern Hemisphere. *Nature Climate Change*, 1.

762 Honda, M., Inoue, J., and Yamane, S. (2009). Influence of low Arctic sea-ice minima on
763 anomalously cold Eurasian winters. *Geophysical Research Letters*, 36(8).

764 Hoshi, K., Ukita, J., Honda, M., Nakamura, T., Yamazaki, K., Miyoshi, Y., and Jaiser, R.
765 (2019). Weak Stratospheric Polar Vortex Events Modulated by the Arctic Sea-Ice
766 Loss. *Journal of Geophysical Research: Atmospheres*, 124(2), 858-869.

767 Hurrell, J. W., and Deser, C. (2010). North Atlantic climate variability: the role of the North
768 Atlantic Oscillation. *Journal of Marine Systems*, 79(3-4), 231-244.

769 Inoue, J., Hori, M. E., and Takaya, K. (2012). The role of Barents Sea ice in the wintertime
770 cyclone track and emergence of a warm-Arctic cold-Siberian anomaly. *Journal of*
771 *Climate*, 25(7), 2561-2568.

772 Jones, P. D., Jonsson, T., and Wheeler, D. (1997). Extension to the North Atlantic Oscillation
773 using early instrumental pressure observations from Gibraltar and south-west
774 Iceland. *International Journal of climatology*, 17(13), 1433-1450.

775 Jung, T., Vitart, F., Ferranti, L., and Morcrette, J. J. (2011). Origin and predictability of the
776 extreme negative NAO winter of 2009/10. *Geophysical Research Letters*, 38(7).

777 Kang, D., Lee, M. I., Im, J., Kim, D., Kim, H. M., Kang, H. S., ... and MacLachlan, C. (2014).
778 Prediction of the Arctic Oscillation in boreal winter by dynamical seasonal forecasting
779 systems. *Geophysical Research Letters*, 41(10), 3577-3585.

780 Kang, W., and Tziperman, E. (2017). More frequent sudden stratospheric warming events due
781 to enhanced MJO forcing expected in a warmer climate. *Journal of Climate*, 30(21),
782 8727-8743.

783 Kelleher, M., and Screen, J. (2018). Atmospheric precursors of and response to anomalous
784 Arctic sea ice in CMIP5 models. *Advances in Atmospheric Sciences*, 35(1), 27-37.

785 King, M. P., Hell, M., and Keenlyside, N. (2016). Investigation of the atmospheric
786 mechanisms related to the autumn sea ice and winter circulation link in the Northern
787 Hemisphere. *Climate dynamics*, 46(3-4), 1185-1195.

788 Kolstad, E. W., and Screen, J. A. (2019). Non-Stationary Relationship between Autumn
789 Arctic Sea Ice and the Winter North Atlantic Oscillation. *Geophysical Research Letters*.

790 Kretschmer, M., Coumou, D., Agel, L., Barlow, M., Tziperman, E., and Cohen, J. (2018).
791 More-persistent weak stratospheric polar vortex states linked to cold extremes. *Bulletin*
792 *of the American Meteorological Society*, 99(1), 49-60.

793 Laloyaux, P., de Boisseson, E., Balmaseda, M., Bidlot, J. R., Broennimann, S., Buizza, R., ...
794 and Kosaka, Y. (2018). CERA-20C: A coupled reanalysis of the Twentieth
795 Century. *Journal of Advances in Modeling Earth Systems*, 10(5), 1172-1195.

796 Luo, D., Chen, Y., Dai, A., Mu, M., Zhang, R., and Ian, S. (2017). Winter Eurasian cooling
797 linked with the Atlantic multidecadal oscillation. *Environmental Research*
798 *Letters*, 12(12), 125002.

799 Luo, D., Chen, X., Overland, J., Simmonds, I., Wu, Y., and Zhang, P. (2019). Weakened
800 potential vorticity barrier linked to recent winter Arctic sea-ice loss and mid-latitude
801 cold extremes. *Journal of Climate*, (2019).

802 McCusker, K. E., Fyfe, J. C., and Sigmond, M. (2016). Twenty-five winters of unexpected
803 Eurasian cooling unlikely due to Arctic sea-ice loss. *Nature Geoscience*, 9(11), 838.

804 Moore, G. W. K., and Renfrew, I. A. (2012). Cold European winters: interplay between the
805 NAO and the East Atlantic mode. *Atmospheric Science Letters*, 13(1), 1-8.

806 Mori, M., Kosaka, Y., Watanabe, M., Nakamura, H., and Kimoto, M. (2019). A reconciled
807 estimate of the influence of Arctic sea-ice loss on recent Eurasian cooling. *Nature*
808 *Climate Change*, 9(2), 123.

809 Orsolini, Y. J., and Kvamstø, N. G. (2009). Role of Eurasian snow cover in wintertime
810 circulation: Decadal simulations forced with satellite observations. *Journal of*
811 *Geophysical Research: Atmospheres*, 114(D19).

812 Orsolini, Y. J., Senan, R., Vitart, F., Balsamo, G., Weisheimer, A., and Doblas-Reyes, F. J.
813 (2016). Influence of the Eurasian snow on the negative North Atlantic Oscillation in
814 subseasonal forecasts of the cold winter 2009/2010. *Climate Dynamics*, 47(3-4), 1325-
815 1334.

816 Orsolini, Y., Wegmann, M., Dutra, E., Liu, B., Balsamo, G., Yang, K., ... and Senan, R.
817 (2019). Evaluation of snow depth and snow-cover over the Tibetan Plateau in global
818 reanalyses using in-situ and satellite remote sensing observations. *The Cryosphere*, 13,
819 2221–2239

820 Overland, J. E., Wood, K. R., and Wang, M. (2011). Warm Arctic—cold continents: climate
821 impacts of the newly open Arctic Sea. *Polar Research*, 30(1), 15787.

822 Overland, J. E., and Wang, M. (2018). Arctic-midlatitude weather linkages in North
823 America. *Polar Science*, 16, 1-9.

824 Pedersen, R. A., Cvijanovic, I., Langen, P. L., and Vinther, B. M. (2016). The impact of
825 regional Arctic sea ice loss on atmospheric circulation and the NAO. *Journal of*
826 *Climate*, 29(2), 889-902.

827 Peings, Y., Brun, E., Mauvais, V., and Douville, H. (2013). How stationary is the relationship
828 between Siberian snow and Arctic Oscillation over the 20th century?. *Geophysical*
829 *Research Letters*, 40(1), 183-188.

830 Peings, Y., Douville, H., Colin, J., Martin, D. S., and Magnusdottir, G. (2017). Snow–(N) AO
831 teleconnection and its modulation by the Quasi-Biennial Oscillation. *Journal of*
832 *Climate*, 30(24), 10211-10235.

833 Peings, Y. (2019). Ural Blocking as a driver of early winter stratospheric
834 warmings. *Geophysical Research Letters*.

835 Petoukhov, V., and Semenov, V. A. (2010). A link between reduced Barents-Kara sea ice and
836 cold winter extremes over northern continents. *Journal of Geophysical Research:*
837 *Atmospheres*, 115(D21).

838 Poli, P., Hersbach, H., Dee, D. P., Berrisford, P., Simmons, A. J., Vitart, F., ... and Trémolet,
839 Y. (2016). ERA-20C: An atmospheric reanalysis of the twentieth century. *Journal of*
840 *Climate*, 29(11), 4083-4097.

841 Rayner, N. A. A., Parker, D. E., Horton, E. B., Folland, C. K., Alexander, L. V., Rowell, D.
842 P., ... and Kaplan, A. (2003). Global analyses of sea surface temperature, sea ice, and
843 night marine air temperature since the late nineteenth century. *Journal of Geophysical*
844 *Research: Atmospheres*, 108(D14).

845 Robinson, David A., Estilow, Thomas W., and NOAA CDR Program (2012). NOAA Climate
846 Data Record (CDR) of Northern Hemisphere (NH) Snow Cover Extent (SCE), Version
847 1.

848 Rohrer, M., Brönnimann, S., Martius, O., Raible, C. C., Wild, M., and Compo, G. P. (2018).
849 Representation of extratropical cyclones, blocking anticyclones, and Alpine circulation
850 types in multiple reanalyses and model simulations. *Journal of Climate*, 31(8), 3009-
851 3031.

852 Rohrer, M., Broennimann, S., Martius, O., Raible, C. C., and Wild, M. (2019). Decadal
853 variations of blocking and storm tracks in centennial reanalyses. *Tellus A: Dynamic*
854 *Meteorology and Oceanography*, 71(1), 1-21.

855 Romanowsky, E., Handorf, D., Jaiser, R., Wohltmann, I., Dorn, W., Ukita, J., Cohen, J.,
856 Dethloff, K. and Rex, M. (2019). The role of stratospheric ozone for Arctic-midlatitude
857 linkages. *Scientific reports*, 9(1), 7962.

858 Ruggieri, P., Kucharski, F., Buizza, R., and Ambaum, M. H. P. (2017). The transient
859 atmospheric response to a reduction of sea-ice cover in the Barents and Kara
860 Seas. *Quarterly Journal of the Royal Meteorological Society*, 143(704), 1632-1640.

861 Saito, K., Cohen, J., and Entekhabi, D. (2001). Evolution of atmospheric response to early-
862 season Eurasian snow cover anomalies. *Monthly Weather Review*, 129(11), 2746-2760.

863 Scaife, A. A., Arribas, A., Blockley, E., Brookshaw, A., Clark, R. T., Dunstone, N., ... and
864 Hermanson, L. (2014). Skillful long-range prediction of European and North American
865 winters. *Geophysical Research Letters*, 41(7), 2514-2519.

866 Scaife, A. A., Karpechko, A. Y., Baldwin, M. P., Brookshaw, A., Butler, A. H., Eade, R., ...
867 and Smith, D. (2016). Seasonal winter forecasts and the stratosphere. *Atmospheric*
868 *Science Letters*, 17(1), 51-56.

869 Scherrer, S. C., Croci-Maspoli, M., Schwierz, C., and Appenzeller, C. (2006). Two-
870 dimensional indices of atmospheric blocking and their statistical relationship with
871 winter climate patterns in the Euro-Atlantic region. *International Journal of*
872 *Climatology: A Journal of the Royal Meteorological Society*, 26(2), 233-249.

873 Schwartz, C., and Garfinkel, C. I. (2017). Relative roles of the MJO and stratospheric
874 variability in North Atlantic and European winter climate. *Journal of Geophysical*
875 *Research: Atmospheres*, 122(8), 4184-4201.

876 Schwierz, C., Croci-Maspoli, M., and Davies, H. C. (2004). Perspicacious indicators of
877 atmospheric blocking. *Geophysical research letters*, 31(6).

878 Screen, J. A. (2017). Simulated atmospheric response to regional and pan-Arctic sea ice
879 loss. *Journal of Climate*, 30(11), 3945-3962.

880 Screen, J. A., Deser, C., Smith, D. M., Zhang, X., Blackport, R., Kushner, P. J., ... and Sun, L.
881 (2018). Consistency and discrepancy in the atmospheric response to Arctic sea-ice loss
882 across climate models. *Nature Geoscience*, 11(3), 155.

883 Smith, D. M., Scaife, A. A., Eade, R., and Knight, J. R. (2016). Seasonal to decadal prediction
884 of the winter North Atlantic Oscillation: emerging capability and future
885 prospects. *Quarterly Journal of the Royal Meteorological Society*, 142(695), 611-617.

886 Sorokina, S. A., Li, C., Wettstein, J. J., and Kvamstø, N. G. (2016). Observed atmospheric
887 coupling between Barents Sea ice and the warm-Arctic cold-Siberian anomaly
888 pattern. *Journal of Climate*, 29(2), 495-511.

889 Sun, C., Zhang, R., Li, W., Zhu, J., and Yang, S. (2019). Possible impact of North Atlantic
890 warming on the decadal change in the dominant modes of winter Eurasian snow water
891 equivalent during 1979–2015. *Climate Dynamics*, 1-11.

892 Suo, L., Gao, Y., Guo, D., Liu, J., Wang, H., and Johannessen, O. M. (2016). Atmospheric
893 response to the autumn sea-ice free Arctic and its detectability. *Climate*
894 *Dynamics*, 46(7-8), 2051-2066.

895 Thompson, D. W., and Wallace, J. M. (1998). The Arctic Oscillation signature in the
896 wintertime geopotential height and temperature fields. *Geophysical research*
897 *letters*, 25(9), 1297-1300.

898 Tibaldi, S., and Molteni, F. (1990). On the operational predictability of blocking. *Tellus*
899 *A*, 42(3), 343-365.

900 Trenary, L., and DelSole, T. (2016). Does the Atlantic Multidecadal Oscillation get its
901 predictability from the Atlantic Meridional Overturning circulation?. *Journal of*
902 *Climate*, 29(14), 5267-5280.

903 Tyrrell, N. L., Karpechko, A. Y., and Räisänen, P. (2018). The influence of Eurasian snow
904 extent on the northern extratropical stratosphere in a QBO resolving model. *Journal of*
905 *Geophysical Research: Atmospheres*, 123(1), 315-328.

906 Tyrrell, N. L., Karpechko, A. Y., Uotila, P., and Vihma, T. (2019). Atmospheric Circulation
907 Response to Anomalous Siberian Forcing in October 2016 and its Long-Range
908 Predictability. *Geophysical Research Letters*, 46(5), 2800-2810.

909 Vihma, T. (2014). Effects of Arctic sea ice decline on weather and climate: A review. *Surveys*
910 *in Geophysics*, 35(5), 1175-1214.

911 Walsh, J. E., Fetterer, F., Scott Stewart, J., and Chapman, W. L. (2017). A database for
912 depicting Arctic sea ice variations back to 1850. *Geographical Review*, 107(1), 89-107.

913 Wang, L., Ting, M., and Kushner, P. J. (2017). A robust empirical seasonal prediction of
914 winter NAO and surface climate. *Scientific reports*, 7(1), 279.

915 Wanner, H., Brönnimann, S., Casty, C., Gyalistras, D., Luterbacher, J., Schmutz, C., ... and
916 Xoplaki, E. (2001). North Atlantic Oscillation—concepts and studies. *Surveys in*
917 *geophysics*, 22(4), 321-381.

918 Warner, J. L. (2018). Arctic sea ice—a driver of the winter NAO?. *Weather*, 73(10), 307-310.

919 Wegmann, M., Orsolini, Y., Vázquez, M., Gimeno, L., Nieto, R., Bulygina, O., ... and Sterin,
920 A. (2015). Arctic moisture source for Eurasian snow cover variations in
921 autumn. *Environmental Research Letters*, 10(5), 054015.

922 Wegmann, M., Brönnimann, S., and Compo, G. P. (2017). Tropospheric circulation during
923 the early twentieth century Arctic warming. *Climate dynamics*, 48(7-8), 2405-2418.

924 Wegmann, M., Y. Orsolini, E. Dutra, O. Bulygina, A. Sterin, and S. Brönnimann, (2017).
925 Eurasian snow depth in long-term climate reanalyses. *Cryosphere*, 11, 923–935

926 Wegmann, M., Orsolini, Y., and Zolina, O. (2018a). Warm Arctic– cold Siberia: comparing
927 the recent and the early 20th-century Arctic warmings. *Environmental Research*
928 *Letters*, 13(2), 025009.

929 Wegmann, M., Dutra, E., Jacobi, H. W., and Zolina, O. (2018b). Spring snow albedo
930 feedback over northern Eurasia: Comparing in situ measurements with reanalysis
931 products. *Cryosphere*, 12(6).

932 Xu, B., Chen, H., Gao, C., Zhou, B., Sun, S., and Zhu, S. (2019). Regional response of winter
933 snow cover over the Northern Eurasia to late autumn Arctic sea ice and associated
934 mechanism. *Atmospheric Research*, 222, 100-113.

935 Yao, Y., Luo, D., Dai, A., and Simmonds, I. (2017). Increased quasi stationarity and
936 persistence of winter Ural blocking and Eurasian extreme cold events in response to
937 Arctic warming. Part I: Insights from observational analyses. *Journal of*
938 *Climate*, 30(10), 3549-3568.

939 Ye, K., & Wu, R. (2017). Autumn snow cover variability over northern Eurasia and roles of
940 atmospheric circulation. *Advances in Atmospheric Sciences*, 34(7), 847-858.

941 Yeo, S. R., Kim, W., and Kim, K. Y. (2017). Eurasian snow cover variability in relation to
942 warming trend and Arctic Oscillation. *Climate dynamics*, 48(1-2), 499-511.

943 Zhang, J., Tian, W., Chipperfield, M. P., Xie, F., and Huang, J. (2016). Persistent shift of the
944 Arctic polar vortex towards the Eurasian continent in recent decades. *Nature Climate*
945 *Change*, 6(12), 1094.

946